JOURNAL OF CATALYSIS 66, 347–367 (1980)

Redox Kinetics of Bismuth Molybdate Ammoxidation Catalysts[1]

JAMES F. BRAZDIL, DEV D. SURESH, AND ROBERT K. GRASSELLI

Department of Research and Development, The Standard Oil Company (Ohio), 4440 Warrensville Center Road, Cleveland, Ohio 44128

Received August 30, 1979; revised July 1, 1980

The response of several bismuth molybdate-based catalysts to reduction under propylene ammoxidation conditions in the absence of gaseous oxygen, and to reoxidation by gaseous oxygen, was studied using a pulse microreactor method. The catalysts investigated were $Bi_2Mo_3O_{12}$, $Bi_2Mo_2O_9$, Bi_2MoO_6, $Bi_3FeMo_2O_{12}$, and a multicomponent system ($M_a^{2+}M_b^{3+}Bi_xMo_yO_z$). The unit area rates of lattice oxygen participation at 430°C decrease in the order: multicomponent system > $Bi_2Mo_2O_9$ > $Bi_2Mo_3O_{12}$ > $Bi_3FeMo_2O_{12}$ ≳ Bi_2MoO_6. Maximum selective utilization of reactive lattice oxygen occurs after partial reduction for the multicomponent system, $Bi_2Mo_3O_{12}$ and $Bi_2Mo_2O_9$. These results are consistent with a mechanism requiring coordinately unsaturated metal ions in complex shear domains for selective ammoxidation. Conversely, $Bi_3FeMo_2O_{12}$ and Bi_2MoO_6 show maximum lattice oxygen activity at their highest oxidation states. The overall reoxidation rates of partially reduced catalysts at 430°C decrease in the order: Bi_2MoO_6 > $Bi_2Mo_2O_9$ > $Bi_2Mo_3O_{12}$ > $Bi_3FeMo_2O_{12}$ ≳ multicomponent system. These reoxidation rates of partially reduced catalysts are first order in oxygen vacancy concentration and half order in gaseous oxygen. A general mechanism for catalyst reoxidation is proposed based on these kinetics. This series of catalysts exhibits two reoxidation regimes. One regime is characterized by a low activation energy at low degrees of initial reduction and involves the reoxidation of surface vacancies. A second regime is observed for deeper degrees of reduction which is characterized by a higher activation energy and involves the reoxidation of anion vacancies in the bulk of the catalyst. The observed activation energies for the reoxidation of the catalyst bulk are strongly dependent upon the structure and composition of the catalyst.

INTRODUCTION

The discovery of bismuth molybdate-based catalysts for the selective (amm)oxidation of propylene (*1*) sparked an extensive research effort to probe the unique properties of these catalytic materials (*2*). Sohio discovered in the early 1950s that these catalysts function through a redox mechanism wherein selective oxidation occurs through loss of lattice oxygen from the bulk structure followed by reduction of gaseous oxygen and bulk transport of oxygen anions to the reduced site. Realization of this redox concept contributed significantly to Sohio's commercialization of (amm)oxidation catalysts (*2*). The unique role of lattice oxygen and not adsorbed oxygen in selective catalytic oxidation has recently been reviewed by Bielanski and Haber (*3*). This redox mechanism has been given formal mathematical treatment by Mars and van Krevelen (*4*).

It has also been found that, although all three phases of bismuth molybdate are selective olefin (amm)oxidation catalysts, there are significant differences in their catalytic activities. These differences have been linked to the relative effectiveness of the redox process which in turn is dependent upon the chemistry and structure of both the surface and the bulk of the catalyst. In order to further understand these differences, it is judicious to separate experimentally the reduction and reoxidation processes and to determine how each in turn contributes to the overall catalytic properties of these systems.

Oxygen depletion and regeneration of

[1] Presented before the Division of Petroleum Chemistry of the American Chemical Society, Washington, D.C., September 1979.

0021-9517/80/120347-21$02.00/0

bismuth molybdate catalysts has been studied using various approaches (*5–10*). In our present study, we used a pulse microreactor (*11, 12*) to obtain quantitative information about the reduction and reoxidation rates of various bismuth molybdate-based catalysts. This method proved desirable since it allows observation of reduction and reoxidation on a shorter time-scale than is otherwise possible. The oxidation state of the catalyst can also be monitored accurately at intervals which are limited only by the size of the pulse. In this manner changes in catalytic activity can be followed during the initial stages of the reaction when the catalyst surface first sees the reactants. Similarly, the reoxidation rate can be accurately determined for various degrees of initial catalyst reduction.

In the work reported here we studied the reduction and reoxidation rates of α-, β-, and γ-bismuth molybdate, single phase $Bi_3FeMo_2O_{12}$, and a multicomponent system ($M_a^{2+}M_b^{3+}Bi_xMo_yO_z$). Each system was shown to be a selective oxidation and ammoxidation catalyst. The ability of each of these systems to use and replenish their lattice oxygens was investigated and the results correlated to the unique structural and chemical properties of these catalysts.

EXPERIMENTAL

Apparatus

The flow diagram for the automated pulse microreactor is shown in Fig. 1. Reactant gases are injected into the reactor from sample loop A which was kept at 47°C and had a constant volume of 0.52 cm^3 (20.2 μmoles). The reaction products were collected in loop B and subsequently injected into the gc for analysis. The Antek 460 gc was equipped with a thermal conductivity detector and a Houdry Micropak system consisting of 36′ × $\frac{1}{16}$″ molecular sieve 5A (45–60 mesh) and 20′ × $\frac{1}{16}$″ Poropak Q (80–100 mesh). The He flow through the columns was held constant at 20 cm^3/min at a head pressure of 56 psig. The system was capable of quantitative separation of propylene, CO_2, O_2, N_2, CO, CH_3CN, acrolein, and acrylonitrile by temperature programming of the gc from 115 to 200°C. Carbon balances of between 95 and 105% were obtainable with this system.

The reactor was a stainless-steel U-tube, composed of a $\frac{1}{8}$″ × 6″ preheat zone and a $\frac{3}{8}$″ × 6″ reactor zone with a maximum catalyst volume of about 5.0 cm^3. The reactor was immersed in a molten salt bath which was temperature controlled at ±0.5°C.

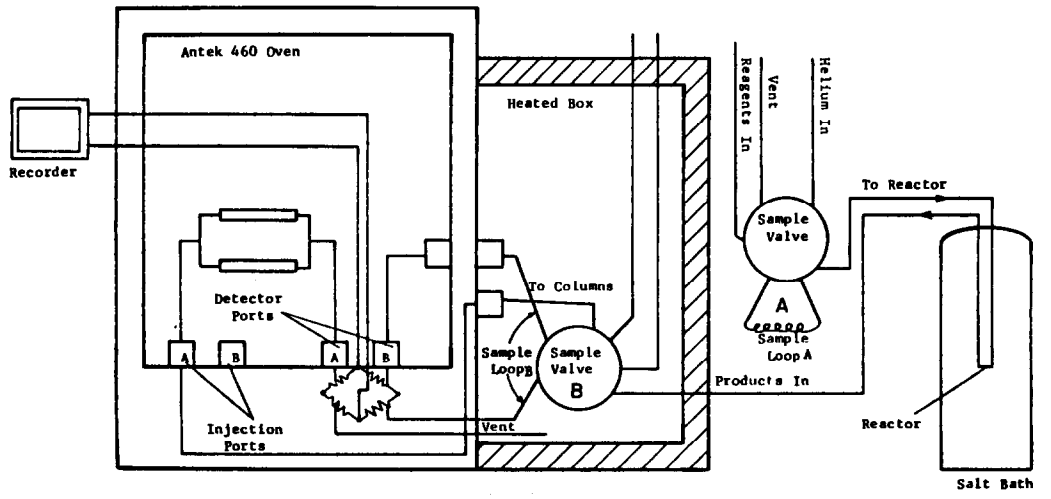

FIG. 1. Schematic diagram of pulse microreactor and gas chromatograph.

The He flow rate over the catalyst was maintained at 24 cm^3/min (measured at 298°K, 1 atm) in all cases. Enough catalyst was used to maintain the contact time at 2.2 sec in all cases.

Experimental Procedure

A summary of the synthetic procedures used to prepare the catalysts for the investigation is given in Table 1. Water was removed from the precipitates by slow evaporation. The phase composition of the calcined catalysts was determined from X-ray powder patterns which compared favorably with those in the literature for each of the molybdate structures indicated. All of the catalysts, with the exception of the multicomponent system, were found to be initially single phase in composition.

The helium used in the pulse microreactor was purified by passing it through a molecular sieve column and through a commercial gas purifier to remove traces of water and oxygen. Oxygen and air were passed through a molecular sieve column prior to use. The propylene and ammonia were obtained from Air Products and were used directly from their cylinder with no additional treatment.

Prior to reduction, the catalysts were pretreated with a 40 cm^3/min flow of air at 430°C for 1 hr. This was done to ensure that the catalyst was completely oxidized at this temperature. It was then immediately placed in an He flow and connected to the pulse gc system, and allowed to equilibrate for about 1 hr.

In order to determine the effect which the 1-hr pretreatment in helium had on the oxidation state of the catalysts, each catalyst was pulsed with a mixture of 20% oxygen in helium at 430°C. The amount of oxygen uptake was then determined for each catalyst. It was found that the pretreatment had no significant effect on the oxidation state of the catalyst since an oxygen uptake of only 0.002×10^{19} [O]/m^2 to 0.006×10^{19}[O]/m^2 was observed. This amounts to about one to two orders of magnitude less than the oxygen removed from the catalysts by a propylene/ammonia pulse as will be shown later.

Reduction of the catalysts was achieved by pulsing with a mixture of 1 propylene/2 ammonia (6.7 μmoles propylene, 13.5 μmoles ammonia per pulse), at 430°C. The extent of catalyst reduction was calculated based on the stoichiometric reaction of propylene and ammonia with lattice oxygen to give the observed product distribution.

Reoxidation of the partially reduced catalysts was accomplished by sequentially pulsing with known mixtures of oxygen and helium at 100-sec intervals. The amount of oxygen uptake by the catalyst during each pulse was calculated from the difference between the initial oxygen content of the pulse and the amount of unreacted oxygen observed in the reactor effluent. The total oxygen vacancy concentration of the partially reduced catalysts was calculated from the total oxygen uptake by the catalyst after sufficient pulsing to give an essentially reoxidized sample. The amount of oxygen uptake agreed well with the calculated amount of oxygen lost during the reducing pulses.

Activation energies for the reoxidation were determined over a temperature range of 320 and 460°C.

Reoxidation Rate Calculations

A pseudo-first-order reoxidation rate constant was calculated from the rate of change of the oxygen vacancy concentration in the catalyst with pulse number. That is:

$$\text{Rate} = k_{app}([O]_V^0 - [O]_i) = \frac{-d[O]_V}{dt_i} \quad (1)$$

where $[O]_v^0$ is the total oxygen vacancy concentration of the catalyst after reduction.

$[O]_i$ is the oxygen uptake by the catalyst after i pulses.

$[O]_v$ is the oxygen vacancy concentration after i pulses which is equal to $[O]_v^0 - [O]_i$.

TABLE 1

Catalyst Preparation and Properties

Catalyst	Preparation[a]	Calcination (°C)	Surface area m^2/g	Density, g/cm^3	Compositions[b]
$Bi_2O_3 \cdot 3MoO_3$	Coprecipitation of MoO_3 dissolved in NH_4OH (ammonium molybdate) and bismuth nitrate in 10% nitric acid solution. Bismuth nitrate solution added to ammonium molybdate solution with stirring	500	1.5	1.14	α-$Bi_2Mo_3O_{12}$[c]
$Bi_2O_3 \cdot 2MoO_3$	Same as $Bi_2O_3 \cdot 3MoO_3$ with ammonium molybdate and bismuth nitrate solutions added simultaneously	500	1.5	1.14	β-$Bi_2Mo_2O_9$[d]
$Bi_2O_3 \cdot MoO_3$	Same as $Bi_2O_3 \cdot 3MoO_3$ with ammonium molybdate solution added to bismuth nitrate solution	500	1.9	1.64	γ-Bi_2MoO_6[c] (Koechlinite)
Multicomponent system	Coprecipitation	500	4.7	0.92	Mixed molybdate phases
$Bi_3FeMo_2O_{12}$	Coprecipitation of ammonium molybdate solution and acidic solution of bismuth and ferric nitrate. pH of slurry adjusted to 4.0 by ammonium hydroxide	500	9.1	1.45	Disordered scheelite[e]
		600	1.8		Ordered scheelite[e]

[a] Catalysts ground and screened to 20–35 mesh particle size.

[b] X-Ray powder pattern.

[c] Aykan, K., *J. Catal.* **12,** 281 (1968).

[d] van den Elzen, A. F., and Riech, G. D., *Mat. Res. Bull.* **10,** 1163 (1975).

[e] Jeitschko, W., Sleight, A. W., McClellan, W. R., and Weiber, J. F., *Acta. Cryst.* **B32,** 1163 (1976).

t_i is the pulse number which is equivalent to a finite time that the catalyst is exposed to the oxidizing gas mixture.

The rate was observed to be first order in the oxygen vacancy concentration from the point where oxygen breakthrough from the reactor occurred to the point of near complete reoxidation of the catalyst. A first-order dependence on the degree of reduction was also observed by Keulks and coworkers (*8, 13*) for the reoxidation of bismuth molybdate.

Under these experimental conditions, the following assumptions are valid:

(i) The catalyst bed is reoxidized uniformly. That is, there is little or no concentration gradient of oxygen vacancies in the bed.

(ii) Changes in the oxygen partial pressure as the pulse moves through the bed are small and thus do not appreciably affect the reaction rate. In this region gaseous oxygen is assumed to be in excess. The rate dependence on oxygen concentration is thus combined with the apparent rate constant and the actual rate expression becomes:

$$\frac{-d[O]_v}{dt_i} = k_{app}[O]_v = k\,[O_2]^n[O]_v \quad (2)$$

where k is the actual reoxidation rate constant and $[O_2]$ is the gas phase concentration of oxygen over the catalyst.

The exact value of n can be determined by varying the partial pressure of oxygen in the pulse and measuring the apparent reoxidation rate constant. A log–log plot of k_{app} versus oxygen partial pressure will yield a straight line with the slope equal to n.

The relative reoxidation abilities of the catalysts were determined by maintaining the initial oxygen concentration of the pulse constant and comparing the observed value of k_{app}.

RESULTS

Reduction

Propylene activity and acrylonitrile yields of the catalysts as a function of the number of propylene–ammonia pulses are illustrated in Figs. 2 and 3, respectively. Since there is no oxygen in the pulses, the reaction proceeds through the removal of

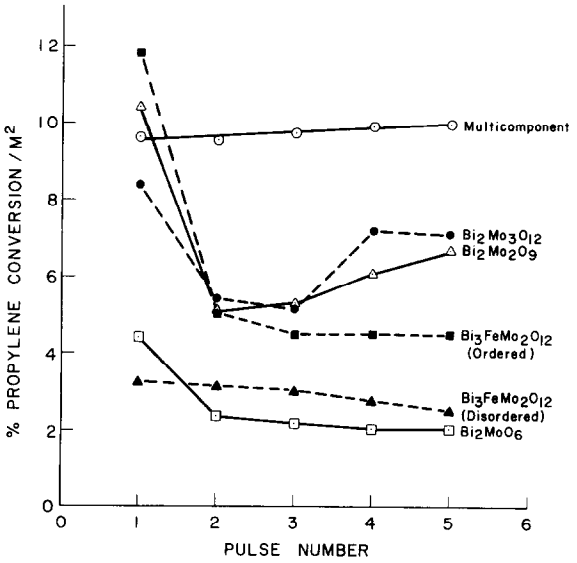

FIG. 2. Propylene conversions during ammoxidation in the absence of gaseous oxygen at 430°C. Catalysts pulsed with a mixture of $1C_3^=/2NH_3$.

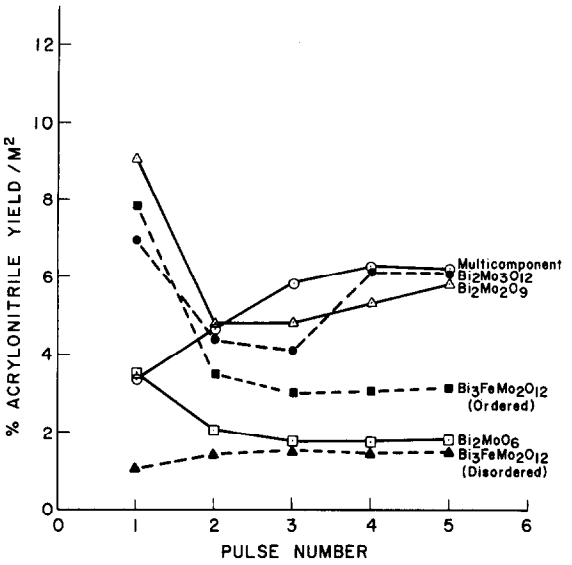

FIG. 3. Acrylonitriles yield during propylene ammoxidation in the absence of gaseous oxygen at 430°C. Catalysts pulsed with a mixture of $1C_3^{2-}/2NH_3$.

lattice oxygens from the catalysts. These plots therefore reflect the trend in catalyst activity with the oxidation state of the catalyst. Typically, the amount of oxygen removal after five reducing pulses ranged between 0.11 and 0.21% of the total oxygen content of the sample. Powder X-ray diffraction experiments did not detect any change in structure of the catalysts after reduction.

In terms of propylene conversion, the γ-phase as well as $Bi_3FeMo_{12}O_{12}$ show maximum activity only when they are near their maximum oxidation state. The depletion of oxygen from the structure results in a lower activity and thus a lower rate of lattice oxygen participation. The loss in activity is probably due to the destruction of the most active surface sites during the first pulse. The sites cannot be readily regenerated by bulk lattice oxygens under anaerobic conditions.

The α- and β-phases also lose activity after the first reducing pulse but regain part of it by the fourth or fifth pulse. The two maxima in activity suggest the existence of two different sites of different oxygen coordination which are capable of selective ammoxidation of propylene.

The multicomponent system showed a monotonic increase in activity reaching a maximum near the fifth reducing pulse.

In all cases further pulsing resulted in a slow drop in catalytic activity due to the progressive loss of oxygen from the catalyst bulk. In this region, a large gradient between the oxygen content of the surface and the bulk is expected, extending many crystallographic layers into the bulk structure. The change in acrylonitrile yield for these catalysts follows the same trends which were observed for the propylene conversion except for the multicomponent system. In this case, maximum acrylonitrile is produced at about the fourth or fifth reducing pulse. This reveals the existence of selective surface sites for this catalyst which are characterized by a lower oxygen coordination or lower oxidation state for the metal ions.

For every catalyst, except the β-phase, these changes in activity and selectivity are the same after the catalysts are reoxidized with gaseous oxygen at 430°C. Reoxidation

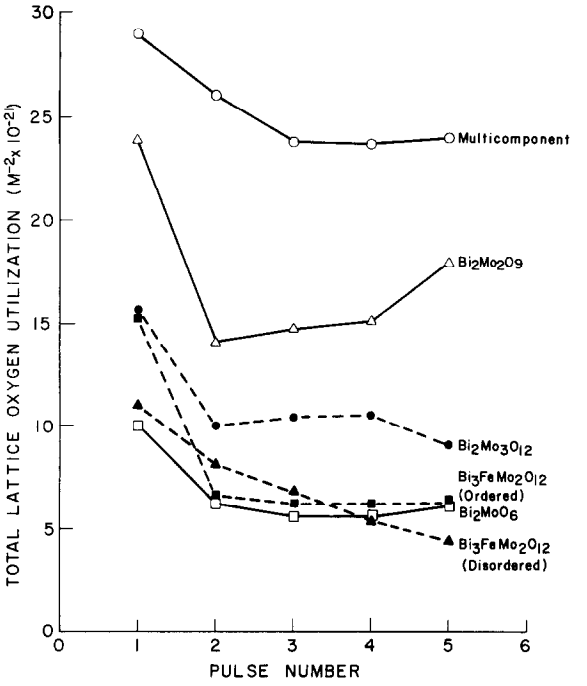

FIG. 4. Total lattice oxygen utilization during propylene ammoxidation in the absence of gaseous oxygen at 430°C.

is therefore able to completely restore the initial states of the catalysts. In marked contrast to this, reoxidation of the β-phase resulted in a catalyst with lower activity than it had initially. After reoxidation, the initial propylene conversion and acrylonitrile yield were about 39% less than that observed in the first reducing cycle. Re-

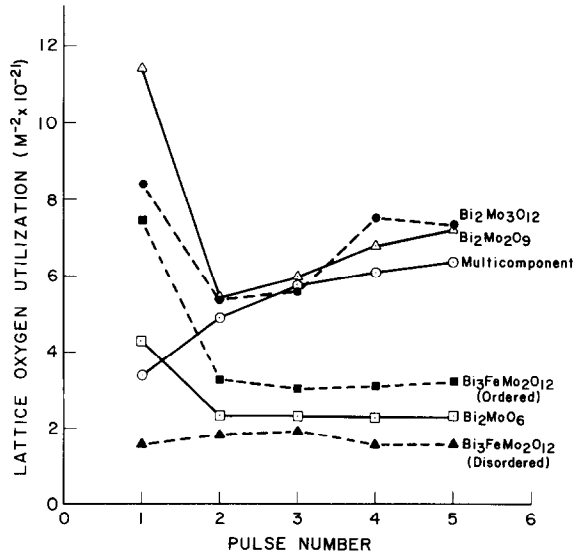

FIG. 5. Selective lattice oxygen utilization for the production of acrylonitrile during propylene ammoxidation in the absence of gaseous oxygen at 430°C.

structuring of the catalyst surface (and bulk) must therefore occur as a result of the reduction/reoxidation cycle.

The above results were used to calculate the distribution of lattice oxygen among the various products and they are summarized in Table 2. The total oxygen utilization by each catalyst is shown in Fig. 4 while Fig. 5 summarizes the change in lattice oxygen utilization for acrylonitrile as a function of catalyst reduction. The rates of lattice oxygen participation during the course of the five reducing pulses are given in Table 3. The values were calculated assuming stoichiometric reaction of lattic oxygen with propylene and ammonia to give the observed product distribution. The results clearly reveal the higher unit surface area activity of the multicomponent system compared to the other catalysts. In sharp contrast to this is the γ-phase which appears to possess a surface with substantially less reactive sites than do the other systems.

In summary, the rates of lattice oxygen participation at 430°C among the catalysts

TABLE 2

Lattice Oxygen Utilization among Products at 430°C[a]

	Pulse number	$CH_2{=}CHC{\equiv}N$ Acrylonitrile	$CH_3C{\equiv}N$	CO	CO_2	N_2	Total [O] lost/m² × 10^{-19}
Multicomponent system	1	0.0339	0.0019	0.0151	0.162	0.0768	0.290
	2	0.0491	0.0030	0.0111	0.125	0.0727	0.261
	3	0.0574	0.0036	0.0039	0.0992	0.0742	0.238
	4	0.0609	0.0039	0.0107	0.0787	0.0673	0.237
	5	0.0637	0.0035	0.0113	0.0761	0.0856	0.240
$Bi_2Mo_3O_{12}$	1	0.0842	0.0071	—	0.0205	0.0446	0.156
	2	0.0538	0.0066	—	0.0073	0.0270	0.0947
	3	0.0559	0.0075	—	0.0075	0.0327	0.104
	4	0.0750	0.0082	—	0.0089	0.0126	0.105
	5	0.0726	0.0072	—	0.0084	—	0.0880
$Bi_2Mo_2O_9$	1	0.114	0.0068	—	0.0196	0.0982	0.239
	2	0.0543	0.0049	—	—	0.0830	0.141
	3	0.0596	0.0059	—	—	0.0819	0.147
	4	0.0676	0.0063	—	0.0005	0.0767	0.151
	5	0.0720	0.0067	—	0.0044	0.0958	0.179
Bi_2MoO_6	1	0.0429	0.0043	—	0.0135	0.0393	0.100
	2	0.0233	0.0025	—	0.0004	0.0356	0.0618
	3	0.0233	0.0024	—	-trace	0.0310	0.0559
	4	0.0228	0.0021	—	-trace	0.0316	0.0565
	5	0.0233	0.0023	—	0.0022	0.0337	0.0615
$Bi_3FeMo_2O_{12}$ (disordered form)	1	0.0154	0.0025	—	0.0915	0.0011	0.1101
	2	0.0182	0.0037	—	0.0573	0.0013	0.0808
	3	0.0192	0.0040	—	0.0440	0.0009	0.0683
	4	0.0155	0.0035	—	0.0334	0.0017	0.0543
	5	0.0156	0.0033	—	0.0241	0.0010	0.0442
$Bi_3FeMo_2O_{12}$ (ordered form)	1	0.0744	0.0158	0.0024	0.0581	0.0020	0.1528
	2	0.0328	0.0080	—	0.0240	0.0015	0.0663
	3	0.0303	0.0071	—	0.0234	0.0011	0.0619
	4	0.0311	0.0069	—	0.0233	0.0010	0.0623
	5	0.0323	0.0069	—	0.0233	0.0010	0.0635

[a] Number of lattice oxygens lost/m², × 10^{-19}.

TABLE 3

Rates of Catalyst Reduction

	Rate of lattice oxygen participation (μmoles [O] lost m^{-2} $pulse^{-1}$)
Multicomponent system	4.11
$Bi_2Mo_3O_{12}$	1.78
$Bi_2Mo_2O_9$	2.44
Bi_2MoO_6	1.07
$Bi_3FeMo_2O_{12}$ (disordered form)	1.17
$Bi_3FeMo_2O_{12}$ (ordered form)	1.26

studied decrease in the following order:

$$\text{Multicomponent system} > Bi_2Mo_2O_9 > Bi_2Mo_3O_{12} > Bi_3FeMo_2O_{12} \geq Bi_2MoO_6.$$

Reoxidation

Apparent first-order reoxidation rate constants were calculated from the change in the oxygen vacancy concentration of the catalyst using Eq. (1). Rate constants were measured over a temperature range of 320 to 460°C and for varying initial degrees of catalyst reduction, and the respective Arrhenius plots are shown in Figs. 6a through e. The activation energies shown in Table 4 were calculated using least-squares linear regression of the data.

Clearly, the activation energies depend upon the initial degree of catalyst reduction. In general at least two reoxidation processes were identified, one with a high rate constant and a low activation energy which usually occurs at low degrees of initial reduction, and a second process for deeper degrees of reduction which is characterized by a lower rate and a higher activation energy. These two processes are further identifiable by the break in the Arrhenius plots for the α- and γ-bismuth molybdates at intermediate degrees of initial reduction (Figs. 6a and c). In these cases, the low energy reoxidation process prevails at higher temperatures (430 to 460°C) while the higher energy process is predominant at lower temperatures (320 to 400°C).

TABLE 4

Activation Energies for Catalyst Reoxidation[a]

Catalyst	Initial ([O] $\times$ $10^{19}/m^2$)	Activation energy (kcal/mole)
$Bi_2Mo_3O_{12}$	0.2	1.3
	0.5	1.4 (430–460°C)
		24.5 (320–400°C)
	1.4	25.9
$Bi_2Mo_2O_9$	0.1	8.1
	0.3	9.6
	0.8	26.6
	1.5	25.8
Bi_2MoO_6	0.2	1.2
	0.5	~0.7 (430–460°C)
		8.1 (320–380°C)
	1.3	7.9
$Bi_3FeMo_2O_{12}$	0.1	4.0
	0.4	6.6
	0.9	8.0
	1.4	8.2
Multicomponent catalyst	0.1	3.6
	0.5	5.2 (430–460°C)
		27.1 (350–400°C)
	1.3	1.4

[a] Temperature range = 320 to 460°C.

The reoxidation processes for the β-phase, $Bi_3FeMo_2O_{12}$, and the multicomponent system are more complex than those observed for the α- and γ-bismuth molybdate. The observed complexities will be discussed in more detail in the following section.

In all cases, the reoxidation rate decreases with an increasing degree of initial catalyst reduction. From the plot (Fig. 7), the reoxidation rates for these catalysts at 430°C decrease in the following order:

$$Bi_2MoO_6 > Bi_2Mo_2O_9 > Bi_2Mo_3O_{12} > Bi_3FeMo_2O_{12} \simeq \text{multicomponent system}$$

The dependence of the reoxidation rate on gaseous oxygen concentration was determined by measuring the pseudo-first-order rate constant at various partial pressures of oxygen in the pulse (Fig. 8). The overall reoxidation rate is about one-half order in oxygen for all the catalysts studied.

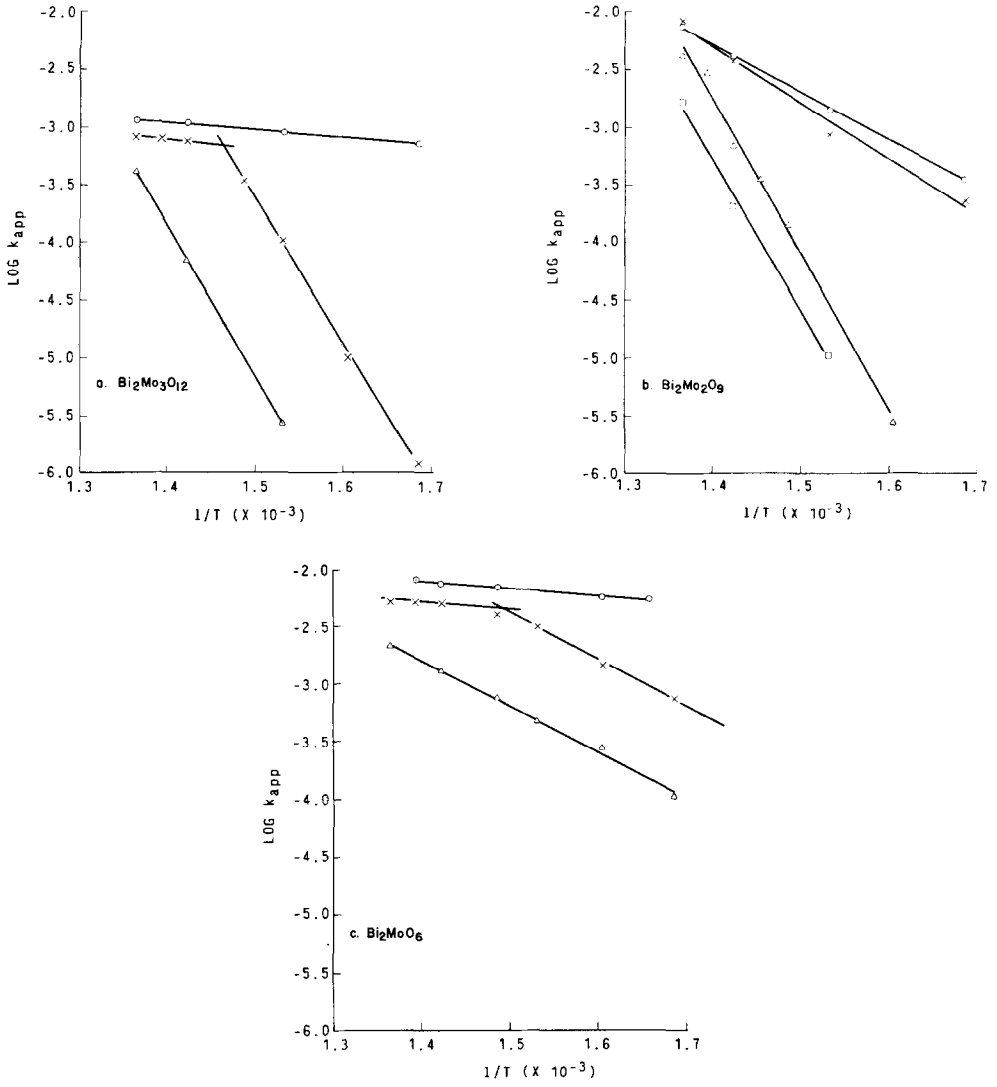

FIG. 6. Temperature dependence of the pseudo-first-order reoxidation rate constant at various degrees of initial catalyst reduction. Catalysts were reoxidized with a mixture of 20 mol% O_2 in He. Temperatures in °K: (a) $Bi_2Mo_3O_{12}$ reoxidized after initial reduction of (○) ~0.2 × 10^{19}[O]/m²; (×) ~0.5 × 10^{19}[O]/m²; (△) ~1.4 × 10^{19}[O]/m². (b) $Bi_2Mo_2O_9$ reoxidized after initial reduction of (○) ~0.1 × 10^{19}[O]/m²; (×) ~0.3 × 10^{19}[O]/m²; (△) ~0.8 × 10^{19}[O]/m²; (□) ~1.5 × 10^{19}[O]/m². (c) Bi_2MoO_6 reoxidized after initial reduction of (○) ~0.2 × 10^{19}[O]/m²; (×) ~0.5 × 10^{19}[O]/m²; (△) ~1.3 × 10^{19}[O]/m². (d) $Bi_3FeMo_2O_{12}$ reoxidized after initial reduction of (○) ~0.1 × 10^{19}[O]/m²; (×) ~0.4 × 10^{19}[O]/m²; (△) ~0.9 × 10^{19}[O]/m² and 1.4 × 10^{19}[O]/m². (e) Multicomponent catalyst reoxidized after initial reduction of (○) ~0.1 × 10^{19}[O]/m²; (×) ~0.5 × 10^{19}[O]/m²; (△) ~1.3 × 10^{19}[O]/m².

In addition, the oxygen dependence remains half order over a wide range of initial degrees of reduction as indicated by the results for the γ-phase in Fig. 8.

DISCUSSION

Catalyst Reduction during Propylene Ammoxidation

The results reported here show that dis-

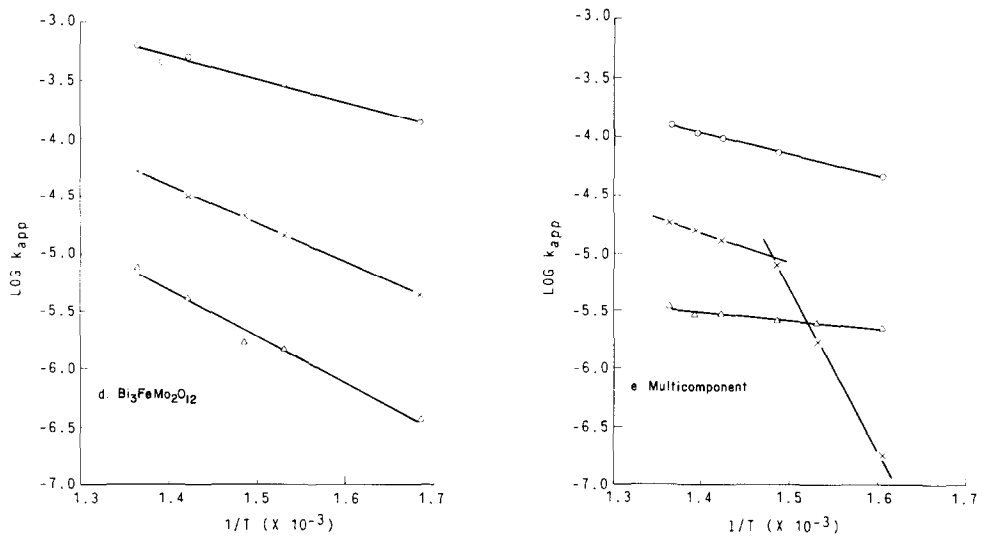

FIG. 6—*Continued.*

tinct changes occur in the catalytic properties of different bismuth molybdate-based systems during the initial stages of catalyst reduction. The most interesting point is the manner in which catalyst behavior is strongly dictated by the structural and chemical make-up of the individual systems. Each catalyst will be discussed in turn to illustrate these points:

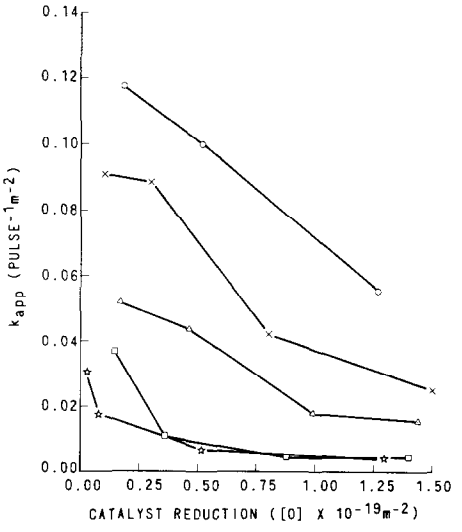

FIG. 7. Dependence of the pseudo-first-order reoxidation rate constant on the initial degree of catalyst reduction for: (○) Bi_2MoO_6; (×) $Bi_2Mo_2O_9$; (△) $Bi_2Mo_3O_{12}$; (□) $Bi_3FeMo_2O_{12}$; and (*) multicomponent catalyst. Catalyst reduction is in units of 10^{19}[O]/m^2 and the reoxidiation rate constants are in units of pulse^{-1} m^{-2}.

γ-Bismuth molybdate. For γ-bismuth molybdate, maximum propylene conversion and acrylonitrile yield occur near its maximum oxidation state (Figs. 2 and 3). It appears, therefore, that the catalytically active site in this system must possess full or nearly full oxygen coordination to be active. Alternatively, it can be said that only a few lattice oxygens surrounding a site for propylene chemisorption are reactive enough to detach from the lattice. Depletion of these oxygens by the first pulse renders some sites inactive. The ability of this catalyst to act as a selective (amm)oxidation catalyst is thus primarily dictated by its ability to regenerate these depleted sites during the reoxidation portion of the redox cycle. Since the active site concentration is relatively low, the reoxidation of the catalyst in the presence of gaseous oxygen must be rapid enough so that chemisorbed propylene and ammonia molecules see an essentially oxidized catalyst surface.

α- and β-Bismuth molybdate. The unique response of the α- and β-phase to reduction during propylene ammoxidation reveals the

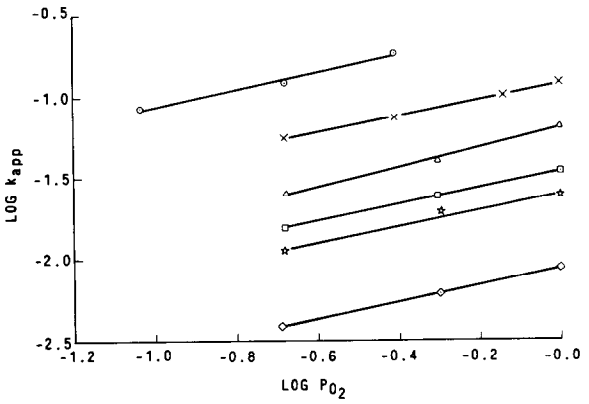

FIG. 8. Straight line fit for the observed dependence of the pseudo-first-order reoxidation rate constant on the partial pressure of oxygen in the reoxidizing pulse at 430°C. The data are for the following catalysts with the indicated initial degrees of catalyst reduction: (○) Bi_2MoO_6, Red. = 0.2×10^{19}[O]/m^2; slope = 0.51; (×) Bi_2MoO_6, Red. = 1.3×10^{19}[O]/m^2; slope = 0.47; (△) $Bi_2Mo_2O_9$, Red. = 1.5×10^{19}[O]/m^2; slope = 0.60; (□) $Bi_2Mo_3O_{12}$, Red. = 1.4×10^{19}[O]/m^2; slope = 0.50; (*) $Bi_3FeMo_2O_{12}$, Red. = 1.4×10^{19}[O]/m^2; slope = 0.49; (◇) multicomponent catalyst, Red. = 1.3×10^{19}[O]/m^2; slope = 0.50.

presence of two distinct regimes where these catalysts are capable of active and selective ammoxidation.

The rapid drop in activity after the first pulse indicates the presence of a catalytic site similar to that observed for γ-bismuth molybdate but with a higher unit surface area concentration (Table 2). This site loses activity as it becomes depleted of oxygens.

After loss of about 0.355×10^{19} lattice oxygens per m^2, the catalytic activity rises to a point approaching that of the completely oxidized system. The amount of lattice oxygens lost in these latter pulses is not much greater than that of the previous pulses (Table 2). However, both the propylene conversion and acrylonitrile yields are observed to increase (Figs. 2 and 3). Examination of the oxygen participation among the products shows that the additional oxygens become available as a result of a decline in the nonselective oxidation of ammonia to N_2 and of propylene to CO_2 (Table 2). This apparently results from an increase in the selectivity of the active sites.

The X-ray diffraction patterns of these reduced systems revealed no bulk structural change which would account for this observation. However, lack of surface sensitivity of these methods does not rule out the possibility of generating a different catalytic phase on the surface as a result of reduction. In any case, these new surface sites can be envisioned as having a lower oxygen coordination on the surface than those of the completely oxidized system. These coordinately unsaturated sites are then capable of more selective oxidation than are the sites with higher oxygen coordination. In other words, propylene reacts and the products are desorbed before complete, nonselective, oxidation can occur. This is a reasonable conclusion since coordinately unsaturated sites are expected to possess metal oxygen bond strengths which are greater than those of a site which possesses its maximum oxygen coordination. Therefore, these more strongly bonded oxygens are expected to be more selective reactants for olefin oxidation than are those which are more loosely bound to the lattice. Multiple oxygen insertion into the chemisorbed propylene is thus less likely to occur. These conclusions reinforce previous observations and hypotheses (*2*, *14*) that

optimally bonded lattice oxygens (i.e., M–O of intermediate bond strengths) are the most selective ones.

The nature of this coordinately unsaturated site can be envisioned as one involving a restructuring of the molybdenum polyhedra (*15, 16*) as shown in Fig. 9. This type of restructuring has been seen on the surface of MoO_3 and WO_3 (*17*). The restructuring allows the solid to accommodate a large number of anion vacancies while maintaining its structural integrity. In relation to catalytic activity, the fully oxidized catalyst is a very active oxidant. The initial loss of oxygen which generates isolated oxygen vacancies diminishes the activity of the catalyst. After the loss of a critical number of oxygens ($\sim 0.355 \times 10^{19}$ $[O]/m^2$ for the α-phase), the molybdenum polyhedra restructure to give complex shear domains in the reduced catalyst. This results in a catalyst which has become more selective due to a slightly higher metal–oxygen bond strength.

Although this surface restructuring can occur as a result of the partial reduction of the catalyst surface, it is likely that this restructured state exists for all active and selective molybdenum catalysts under steady-state reaction conditions. Under such conditions, the restructuring can be essentially instantaneous and not readily observed by any changes in the catalytic activity and selectivity.

$Bi_3FeMo_2O_{12}$—disordered and ordered scheelite phases. The incorporation of iron into the scheelite structure of α-bismuth molybdate has been shown to result in a single phase system of composition $Bi_3FeMo_2O_{12}$ (*18*). The phase is formed from the $Bi_2Mo_3O_{12}$ structure by isomorphous replacement of Mo by an Fe atom in the B (tetrahedral) site on the ABO_4 scheelite with the additional bismuth taking

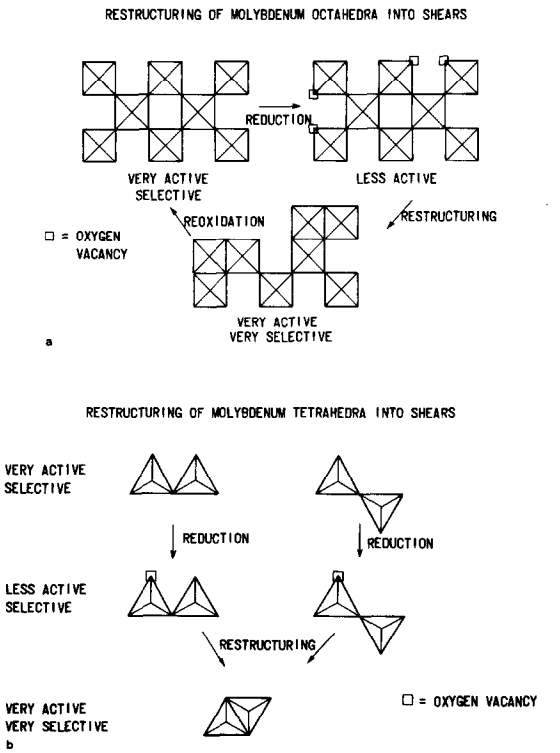

FIG. 9. Shear formation in molybdenum polyhedra for (a) molybdenum octahedra and for (b) molybdenum tetrahedra.

up the single cation vacancy. The system was found to exist in two forms: a high-temperature ordered form and a low-temperature disordered form (*18*).

Comparison of the unit surface activity of these two forms (Table 2) shows that both have similar activity. The selectivity of the ordered form is, however, somewhat higher than the disordered one. This may be due to the presence of lower coordinated iron in the ordered form (*18*). The resultant higher metal oxygen bond strength would thus favor selective (amm)oxidation over nonselective (amm)oxidation.

The decline in activity with degree of reduction for the $Bi_3FeMo_2O_{12}$ phase (Figs. 2 and 3) indicates that its surface catalytic activity is quite similar to that of γ-bismuth molybdate. In other words, rapid regeneration of the depleted surface oxygens during the reoxidation cycle is necessary to maintain its highest activity. The unusual similarity of these two catalysts will be further discussed in the context of their reoxidation abilities.

$M_a^{2+}M_b^{3+}Bi_xMo_yO_z$ multicomponent system. The unit surface area activity of the multicomponent system was substantially higher than any of the other systems investigated (Table 3). Propylene conversion remained fairly constant throughout the five reducing pulses (Fig. 2). In sharp contrast to the results obtained for the other catalysts, the multicomponent system reached its maximum selectivity to AN only after the loss of about 1×10^{19} oxygens per unit surface area (Fig. 3). Although the total amount of reactive oxygens decreases slightly during the reduction (from $\sim 0.29 \times 10^{19}$[O]/m^2 to $\sim 0.24 \times 10^{19}$[O]/m^2 lost), the yield of acrylonitrile increased. The additional lattice oxygens for the selective ammoxidation resulted from the decrease in the nonselective oxidation of propylene to CO_2 and CO (Table 2).

It appears from these results that it is primarily the nature of the active surface site which changes in this catalyst reduction. The continuous increase in selectivity indicates that it is not the destruction of one type of surface site followed by the appearance of a new more selective one which is occurring. Rather, it is the transformation of an initially nonselective site to a more selective one which takes place. The most selective sites on the surface of this catalyst are, therefore, those which possess a certain degree of anion vacancy and coordinate unsaturation of the metal ions. This result is consistent with the theory of site isolation previously proposed (*14*) where the degree of oxygen coordination around a given metal atom site dictates whether the site will be selective or nonselective. In the case of the multicomponent system, high oxygen coordination causes multiple insertion of lattice oxygens into the chemisorbed propylene resulting in nonselective oxidation of CO_2. The coordinately unsaturated site permits desorption of acrylonitrile before complete oxidation can occur.

This more selective site can be viewed as resulting from the restructuring of the molybdenum polyhedra into shear planes as was discussed earlier for the α- and β-phases.

In the multicomponent system, complete reoxidation of the active site is not necessary to maintain high activity and selectivity. A balance must therefore be kept between the oxidation state of the surface and the rate of reoxidation in order to maintain this maximum selectivity under steady-state conditions.

Catalyst Reoxidation

Mechanism. The overall rate expression for catalyst reoxidation is given by Eq. (2) where n is equal to 1/2. This rate expression can be explained by the following general mechanism:

$$M + O_2 \rightleftharpoons M\text{–}O_2 \quad (3)$$

$$M\text{–}O_2 + M \rightleftharpoons M\text{–}O + M\text{–}O \quad (4)$$

$$M\text{–}O + V \rightarrow O\ (\text{lattice}) + M \quad (5)$$

M represents surface sites where gaseous oxygen is chemisorbed and dissociated, and V represents anion vacancies either on

the surface or in the bulk, where the newly incorporated oxygen finally resides in the lattice. Step 1 represents the reversible adsorption of dioxygen followed by Step 2, the oxygen dissociation. Because of the half order dependence in oxygen, both steps must occur prior to the rate-determining Step 3. The rate-limiting step involves the incorporation of oxygen into an anion vacancy. If the anion vacancy is located in the bulk of the catalyst, the rate of Step 3 may be further limited by the oxygen diffusion properties of the solid.

Physically, the initial steps of adsorption and dissociation of dioxygen can be viewed as taking place on coordinately unsaturated metal cations on the surface. These cations serve as the reoxidation centers for the catalyst and must, according to the general redox mechanism, be physically removed from the centers which activate the hydrocarbon. A more precise picture of the adsorption and dissociation during catalyst reoxidation is provided in the following two mechanistic schemes:

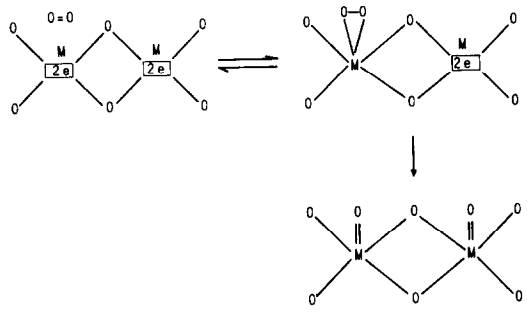

SCHEME 1

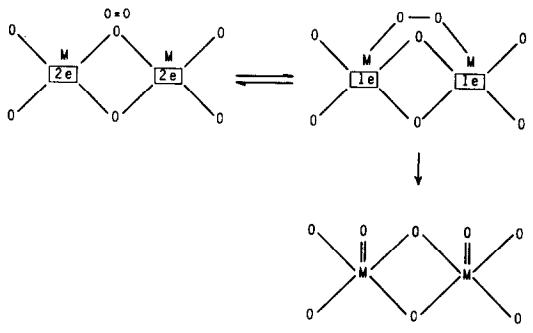

SCHEME 2

In Scheme 1, dioxygen is adsorbed onto a single coordinately unsaturated metal cation on the surface of the reduced catalyst forming a peroxo surface species. An end-on interaction between the dioxygen and the metal which produces a "charged" oxygen radical is also a possibility. This, however, is less likely to be an intermediate for reoxidation for two reasons: (i) The O–O distance in the peroxo species is typically 1.40 to 1.5 Å whereas for the oxygen radical, it is usually 1.30 to 1.35 Å in transition metal complexes (*19*). The peroxo complex is thus more likely to lead to the dissociated oxygen species required to occupy the anion vacancies in the reduced catalyst. (ii) Numerous studies have failed to show the existence of oxygen radicals on the surface of any bismuth molybdate catalyst even though they are readily observed on other transition metal oxides (*3*). This fact suggests the existence of a covalent peroxo species rather than an ionic intermediate.

After coordination, the dioxygen is dissociated on a second surface cation which may or may not be the same type as the first. These oxygens then diffuse to existing anion vacancies on the surface or in the bulk. This process then regenerates the reoxidation center on the catalyst surface.

A second possible mechanism, for reoxidation is shown in Scheme 2. In this case, dioxygen coordinates symmetrically to two close-lying coordinately unsaturated surface cations forming a covalent oxygen bridge between the two centers. Just as in the case of the peroxo intermediate, dissociation of the bridging oxygen is expected to be an easy process at high temperatures. The dissociated oxygen can then readily diffuse to the anion vacancies in the lattice.

Whether or not a peroxo or a bridging species is the most likely intermediate in the reoxidation of a bismuth molybdate catalyst depends upon both topographical and electronic factors. Obviously, the formation of the bridged species requires that two metal centers with the correct oxidation potential be in close enough proximity

on the surface. This is a stringent requirement which may not always be possible on all catalysts. In addition, the ease with which the cations can transfer electrons to the oxygen molecule in one of these complexes is also of paramount importance. Because the reduction of an O_2 molecule requires the transfer of four electrons, the symmetrical bridged intermediate is in some ways more appealing. In this case, each metal center can simultaneously perform two one-electron transfers to the oxygen molecule. The insertion of another metal center into an existing dioxygen intermediate is not required as it is in Scheme 1. Nevertheless for any given catalyst which operates by a redox process, reoxidation may in fact occur by both mechanisms simultaneously. The relative contribution from each mechanism will be dictated by the structure and chemical composition of the catalyst surface and bulk.

The exact chemical make-up of the reoxidation site on a bismuth molybdate catalyst has not yet been clearly demonstrated. However, for the reoxidation mechanisms proposed here, it seems likely that at least one of the metal centers may be a reduced molybdenum cation. Molybdenum is known to form various multivalent coordinate compounds containing oxygen (*19, 20*). Since molybdenum is also stable in its lower valence states, it seems likely that such centers can serve as the sites for the initial reduction of dioxygen. Reoxidation rate studies on simple bismuth and molybdenum oxides which help clarify this point will be reported in a forthcoming paper.

Reoxidation of α- and γ-bismuth molybdates. Two reoxidation processes were observed for the α- and γ-bismuth molybdate phases which are a function of the initial degree of catalyst reduction. At low degrees of reduction (lattice oxygen removal of about 0.2×10^{19}[O]/m^2), the reoxidation of these catalysts proceeds with an activation energy of about 1.2 and 1.3 kcal/mole. Reoxidation in this case is confined primarily to the surface region of the catalyst. The activation energy is low for this process since only surface diffusion of oxygen is required to fill oxygen vacancies in the catalyst. These results also indicate that the chemisorption and dissociation of dioxygen on a reduced bismuth molybdate surface occurs quite readily. The relatively high reoxidation rate at this level of initial reduction indicates that regeneration of the reoxidation site is rapid. The similarity in the activation energies for these two catalysts, under conditions where the reoxidation is surface limited, suggests that their reoxidation sites are quite similar.

When the initial reduction of the catalyst was extended to about 1.4×10^{19}[O]/m^2, the activation energy for the reoxidation increased. For the α-phase, the activation energy increased to about 26 kcal/mole whereas for the γ-phase the increase was only to about 8 kcal/mole. This observed difference in activation energies results under deeper reduction conditions, because now reoxidation of the catalyst involves subsurface vacancies and not just the surface. The reoxidation rate is therefore limited by the intrinsic ability of the catalysts to transport the newly incorporated surface oxygens away from the reoxidation sites and to the vacancies in the bulk structure.

This lattice diffusion is apparently a much easier process in the γ-phase than it is in the α-phase. The reason for this can be surmised from the structural features of the γ-phase (*21, 22*). This phase has been shown to contain alternating layers of O^{2-} oxygen anions which separate neighboring Bi_2O_2 and MoO_2 layers. These layers of oxygen anions can serve as facile routes for oxygen diffusion within the bulk structure. The α-phase contains no such structural pathways and is in fact a more closed packed structure than is the γ-phase (*23*). Since, as mentioned above, the energy for chemisorption and dissociation of dioxygen is apparently similar for both phases, the observed differences in activation energies are a result of the relative abilities of these

catalysts to transport oxygen anions from the reoxidation site to bulk anion vacancies. The γ-phase is thus better suited structurally for this diffusion process.

Another important point of comparison are the relative ratios of the reduction rates and the reoxidation rates of these catalysts (Table 5). The results suggest that the α-phase has either a higher concentration of active sites on the surface than does the γ-phase or that the concentration of sites is similar but site reconstitution is faster for the α-phase. It is not possible at present to distinguish between these two possibilities clearly. However, in the case of reoxidation it appears that the reoxidation sites for the γ-phase are more efficient than they are for the α-phase. Rapid diffusion of oxygen anions away from the reoxidation sites results in a faster regeneration of reoxidation sites on the surface of γ-bismuth molybdate.

At intermediate degrees of reduction (lattice oxygen removal of about 0.5×10^{19}[O]/m^2), both processes can be observed depending upon the reoxidation temperature (Figs. 6a and c). At low temperatures, below about 410°C, the reoxidation rate is diffusion limited in both the α- and γ-phases. The calculated activation energies in this regime are very characteristic of the previously observed diffusion limited reoxidation processes for these catalysts: about 25 kcal/mole for the α-phase and about 8 kcal/mole for the γ-phase. When these catalysts are reoxidized at higher temperatures, i.e., between 430 and 460°C, the rate is no longer diffusion limited. Instead, the observed activation energies are similar to those observed for the reoxidation of surface oxygen vacancies on these catalysts.

TABLE 5

Reduction/Reoxidation Rate Ratios at 430°C

Catalyst	k_{red}/k_{reox} ([O] pulse^{-1} m^{-2})
Multicomponent catalyst	587.1
$Bi_3FeMo_2O_{12}$	106.4
$Bi_2Mo_3O_{12}$	40.7
$Bi_2Mo_2O_9$	57.8
Bi_2MoO_6	10.7

At this intermediate level of reduction, oxygen vacancies are apparently generated both on the surface and in the bulk of the catalysts. At low temperatures surface oxygen anions must overcome the diffusional barrier in the solid in order to occupy these subsurface vacancies. At the higher temperatures, the mobility of these vacancies increases. As a result, they may tend to concentrate on the catalyst surface. Reoxidation then is no longer diffusion limited but instead proceeds by the low energy path involving only the surface region of the catalyst.

Reoxidation of β-bismuth molybdate. The Arrhenius plot for the reoxidation of the β-phase (Fig. 6b) shows no evidence of a low energy surface reoxidation process like that observed for the α- and β-phases. Instead the observed activation energies are very characteristic of the diffusion limited reoxidation of either α- or γ-bismuth molybdate. When the initial reduction was about 0.3×10^{19}[O]/m^2, the activation energy for reoxidation was about 8 to 9 kcal/mole for this catalyst. This level of reduction in the α- and γ-phases resulted in an oxygen loss from only the surface region of the catalyst. If a similar situation existed for the β-phase, a much lower activation energy would be expected for a single phase system. The observed activation energy instead indicates that the catalyst surface consists primarily of a reduced γ-phase under these conditions.

When the initial degree of reduction was increased into the range 0.8×10^{19}[O]/m^2 to 1.5×10^{19}[O]/m^2, the observed activation energy for reoxidation increased markedly to a value of about 26 kcal/mole. This activation energy is the same as that observed previously for the reoxidation of the α-phase. This strongly suggests that at this level of reduction, the oxygen re-

moval from the catalyst extends beyond the surface layer to a subsurface region which consists, at least in part, of α-bismuth molybdate.

The existence of both α- and γ-bismuth molybdate on the catalyst can be visualized as arising from the disproportionation of the β-phase during reduction as follows:

$$Bi_2Mo_2O_9\ (\text{surf.}) \xrightarrow{\text{Reduction}} Bi_2MoO_{6-x}\ (\text{surf.}) + MoO_{3-y} + (x + y)\ [O]$$

$$Bi_2Mo_2O_9\ (\text{bulk}) + MoO_{3-y} \rightarrow Bi_2Mo_3O_{12-y}\ (\text{bulk})$$

$$Bi_2MoO_{6-x}\ (\text{surf.}) + \frac{x}{2} O_2 \xrightarrow{\text{Reoxidation}} Bi_2MoO_6\ (\text{surf.})$$

$$Bi_2Mo_3O_{12-y}\ (\text{bulk}) + \frac{y}{2} O_2 \xrightarrow{\text{Reoxidation}} Bi_2Mo_3O_{12}\ (\text{bulk})$$

It is possible that the free molybdenum oxide on the surface will not migrate into the bulk of the catalyst but will instead sublime off the surface. Then, the 26 kcal/mole activation energy observed for the reoxidation is the result of a diffusion limited process for the β-bismuth molybdate phase and not for the α-phase. However, there is little reason to expect that both bismuth molybdate phases would have identical activation energies since the diffusion-limited reoxidation process is sensitive to the bulk structure of the catalyst. Therefore, the mechanism proposed above appears to be a reasonable one.

The disproportionation mechanism given above is supported by the change in initial activity during the pulse reduction. As mentioned before, the β-phase was the only catalyst which experienced a step decline in its initial activity after the first reduction–reoxidation cycle. This is consistent with the proposed existence of a surface layer of the γ-phase since this phase was observed to have the lowest rate of lattice oxygen participation.

The stability of the β-bismuth molybdate phase has been suspect in earlier studies (*24*). A recent examination by transmission electron microscopy (*25*) concluded that this catalyst thermally decomposes into the γ-phase and MoO_2 in both a vacuum and in an oxygen atmosphere. From our investigation, it appears that significant disproportionation occurs only after the catalyst is contacted with the reactant gas mixture. Simple thermal decomposition would be expected to result in a lower initial activity than was observed during the pulse reduction with propylene and ammonia. Instead, the step change in catalyst activity occurred only after the completion of a reduction–reoxidation cycle. These results suggest that this catalyst will readily disproportionate on the surface under reaction conditions. This makes any "steady state" kinetic information about the β-phase suspect.

Reoxidation of $Bi_3FeMo_2O_{12}$. The incorporation of iron into the scheelite structure of α-bismuth molybdate can be seen to dramatically change its reoxidation properties. First of all, the activation energy for reoxidation after high levels of initial reduction (i.e., at 0.9×10^{19}[O]/m^2 and 1.4×10^{19}[O]/m^2) is reduced by about a factor of three compared to α-bismuth molybdate (Table 4). This level of reduction is expected to result in oxygen removal beyond the surface layers of the catalyst as was observed for both α- and γ-bismuth molybdate. Reoxidation under these conditions must therefore be in a diffusion-limited regime since oxygen has to be transported from the surface to the anion vacancies in the bulk. The incorporation of iron into the scheelite structure aids this transport of oxygen in the catalyst. The role of iron can be viewed as enhancing the electron transport in the catalyst by the presence of interlinking Fe^{2+}/Fe^{3+} redox couples in the partially reduced catalyst. The surface reoxidation sites can be rapidly regenerated by this process since electron transfer to these sites is facilitated by the iron. In fact, iron may also be an important constituent of

the reoxidation site for this catalyst. Ferrous cations at the surface can readily pick up gaseous oxygen and transfer it to underlying cations in the bulk with the subsequent regeneration of the reoxidation site. The facile interchange between Fe^{2+} and Fe^{3+} results in a low energy path for reoxidation of the catalyst bulk and in the rapid reconstitution of the reoxidation site.

Although the activation energy for reoxidation of $Bi_3FeMo_2O_{12}$ is less than that for α-bismuth molybdate, the absolute rate of reoxidation is not higher. The reason for this is that the major role of iron in the structure is to enhance the activity of the active sites. This is apparent (Table 5) by comparing the ratio of the unit surface area reduction rate to the reoxidation rate for $Bi_3FeMo_2O_{12}$ which is nearly three times that of α-bismuth molybdate. Although the unit surface area concentration of reoxidation sites is significantly less for $Bi_3FeMo_2O_{12}$, the presence of iron enhances the efficiency of these sites.

For very low levels of initial reduction (oxygen loss of 0.15×10^{19}[O]/m^2), the observed activation energy of 4 kcal/mole for the reoxidation $Bi_3FeMo_2O_{12}$ is greater than that for the reoxidation of surface vacancies (Table 4). Although lower than the 7 to 8 kcal/mole observed for deeper degrees of initial reduction, it still must correspond to a process involving the reoxidation of at least some bulk oxygen vacancies in the catalyst. It appears, therefore, that after reduction the surface of the $Bi_3FeMo_2O_{12}$ catalyst is rapidly reoxidized by lattice oxygens in the bulk. Iron helps to maintain the catalysts surface in a relatively high oxidation state. During reoxidation then, gaseous oxygen which is chemisorbed and dissociated at the surface, must be incorporated into these anion vacancies in the bulk even when the initial level of catalyst reduction is very low.

Reoxidation of multicomponent system ($M_a^{2+}M_b^{3+}Bi_xMo_yO_z$). The Arrhenius plot shown in Fig. 6e reveals that the reoxidation processes of the multicomponent catalyst are quite complex.

At low levels of initial reduction, corresponding to an oxygen loss of about 0.1×10^{19}[O]/m^2, the catalyst behaves much like the $Bi_3FeMo_2O_{12}$ system. The surface of the catalyst appears to be rapidly reoxidized by lattice oxygen from the bulk after contact with propylene and ammonia. The reoxidation of the catalyst by gaseous oxygen proceeds by a mechanism which transports oxygen from the reoxidation site to vacancies in the bulk. The activation energy for the process is quite low at 3.6 kcal/mole and is similar to that observed for $Bi_3FeMo_2O_{12}$ under the same conditions.

At an initial reduction of about 0.5×10^{19}[O]/m^2, two reoxidation processes are apparent which are a function of the temperature of reoxidation. At temperatures between about 420 and 460°C, the activation energy is only about 5 kcal/mole. For reoxidation temperatures between 320 and 400°C, the activation energy increases markedly to 27 kcal/mole. This high activation energy is indicative of a diffusion-limited reoxidation process wherein oxygen anions moving from the surface to the bulk must overcome a large energy barrier. This energy barrier probably has its origin in the structural nature of the catalyst as was observed for α-bismuth molybdate.

When the multicomponent catalyst is reduced deeper to a level of 1.3×10^{19}[O]/m^2, the activation energy for the reoxidation of the catalyst was found to be only 1.4 kcal/mole. This low activation energy must result from the creation of a new pathways for the reoxidation of the catalyst bulk due to the depletion of oxygen from the lattice. As discussed previously, reduction of the multicomponent system can produce shear domains in the structure. Oxygen anions are expected to be able to diffuse quite readily along these sheer dislocations. They can therefore serve as low-energy pathways for the transport of oxygen from a surface reoxidation site to an oxygen vacancy in the catalyst bulk.

CONCLUSIONS

Our pulse microreactor study of the redox properties of various bismuth molybdate-based ammoxidation catalysts reveals that the effectiveness of the redox process is strongly dependent upon the structure and composition of the catalyst. The multicomponent catalyst is the most active for propylene ammoxidation in the absence of gaseous oxygen. The high activity results from a large concentration of propylene chemisorbing sites which are rapidly reconstructed by lattice oxygen from the bulk.

The ability of a catalyst to reconstruct effectively after partial reduction is an important contributor to selectivity. Restructuring can result in the formation of complex shear domains due to the collapse of molybdenum polyhedra from corner to edge sharing after the creation of a critical number of oxygen vacancies. Shearing produces surface sites with an optimum metal oxygen bond strength which makes multiple oxygen insertion into the chemisorbed propylene less likely. Shearing can also aid in the reconstitution of active sites by enhancing the mobility of oxygen anions from the bulk to surface sites. Catalyst structures with relatively high molybdenum contents (notably the multicomponent catalyst, α- and β-bismuth molybdate) are uniquely able to reconstruct after partial reduction. The γ-bismuth molybdate and $Bi_3FeMo_2O_{12}$ structures are not able to restructure and thus possess maximum lattice oxygen activity only at their highest oxidation state.

The observed kinetics for catalyst reoxidation can be explained by a general mechanism involving the reversible adsorption of dioxygen followed by dissociation on the surface. The rate-limiting step is the incorporation of the dissociated oxygen into vacancies on the surface or in the bulk. It is proposed that the initial stage of reoxidation proceeds via either a peroxo or an oxygen bridged-type surface intermediate (Schemes 1 and 2).

In general two regimes for catalyst reoxidation are observed. The reoxidation of vacancies at the surface is relatively fast and proceeds with an activation energy barrier of only 1 to 2 kcal/mole. The reoxidation of vacancies in the bulk is a higher energy process and is limited by the ability of the catalyst to transport oxygen from the surface to the bulk. Layering in the γ-bismuth molybdate structure results in low energy pathways for the diffusion of oxygen anions and oxygen vacancies. In more close-packed structures like α- and β-bismuth molybdate the oxygen mobility is low and the overall reoxidation rate is slower. The presence of a redox couple in the catalyst however can promote electron and oxygen transfer. Iron in the $Bi_3FeMo_2O_{12}$ scheelite structure promotes the rapid exchange of oxygen between the reoxidation sites and the bulk by means of interlinking Fe^{3+}/Fe^{2+} redox couples in the partially reduced catalyst. The oxygen mobility in the multicomponent system is enhanced by the presence of shear structures in the lattice. The multicomponent catalyst is unique in that particularly facile pathways of oxygen transfer, site reconstruction, and electron exchange are available to it.

ACKNOWLEDGMENTS

We would like to acknowledge Dr. J. D. Burrington for helpful discussions and Mr. M. J. Seely for carrying out part of the experimental work.

REFERENCES

1. Idol, J. D. (to Sohio), U.S. Patent 2,094,580 (September 15, 1959); Callahan, J. L., and Gertisser, B. (to Sohio), U.S. Patent 3,198,750 (August 3, 1965); Callahan, J. L., and Gertisser, B. (to Sohio), U.S. Patent 3,308,151 (March 7, 1969); Grasselli, R. K., and Hardman, H. F., U.S. Patent 3,642,930 (February 15, 1972).
2. Callahan, J. L., Grasselli, R. K., Milberger, E. C., and Strecker, H. A., *I EC Prod. Res. Dev.* **9**, 134 (1970) and references therein.
3. Bielanski, A., and Haber, J., *Catal. Rev. Sci. Eng.* **19**, 1 (1979).
4. Mars, P., and van Krevelen, D. W., *Chem. Eng. Sci. Suppl.* **3**, 41 (1954).

5. Yong, L. K., Howe, R. F., Keulks, G. W., and Hall, W. K., *J. Catal.* **52,** 544 (1978).
6. Ruckenstein, E., Krishnan, R., and Rai, K. N., *J. Catal.* **45,** 270 (1976).
7. Dadyburjor, D. B., and Ruckenstein, E., *J. Phys. Chem.* **82,** 1563 (1978).
8. Monnier, J. R., and Keulks, G. W., Presented before the Division of Petroleum Chemistry, Inc. at the Joint Meeting of the A.C.S. and the Chemical Society of Japan (April 1–6, 1979), Honolulu, Hawaii.
9. Matsuura, I., and Schuit, G. C. A., *J. Catal.* **20,** 19 (1971); *J. Catal.* **25,** 314 (1972).
10. Keulks, G. W., and Krenzke, L. D., *Proc. Sixth Int. Congr. Catal.* **2,** 806 (1977).
11. Bassett, D. W., and Habgood, H. W., *J. Phys. Chem.* **64,** 769 (1960).
12. Blanton, W. A., Byers, C. H., and Merrill, R. P., *I EC Fund.* **7,** 611 (1968).
13. Keulks, G. W., and Daniel, C., Presented at the Symposium on the Role of Solid State Chemistry in Catalysis (March 21–25, 1977), New Orleans, Louisiana.
14. Callahan, J. L., and Grasselli, R. K., *A.I.Ch.E. J.* **9,** 755 (1963).
15. Grasselli, R. K., Presented at the Advances in Oxidation Chemistry Series (April 1975), University of Manchester, U.K.
16. Stone, F. S., *J. Solid State Chem.* **12,** 271 (1972).
17. Gai, P. L., Proceedings Third Int. Conf. on the Chemistry and Uses of Molybdenum, p. 143 (August 1979).
18. Jeitschko, W., Sleight, A. W., McClellan, W. R., and Weiber, J. F., *Acta Cryst.* **B32,** 1163 (1976); Sleight, A. W., and Jeitschko, W., *Mat. Res. Bull.* **9,** 951 (1972); Linn, W. J., and Sleight, A. W., *J. Catal.* **41,** 134 (1976).
19. Ugo, R., *Coll. Int. CNRS* **281,** 133 (1977).
20. Spitsyn, V. I., Subbotina, N. A., Felin, M. G., Pakhomov, S. I., and Zhirov, A. I., *Dokl. Chem.* **245,** 185 (1979).
21. Zemann, J., *Heidelberger Beitr. Miner. Petr.* **5,** 139 (1956).
22. Van den Elzen, A. F., and Rieck, G. D., *Acta. Cryst.* **B29,** 2436 (1973).
23. Van den Elzen, A. F., and Rieck, G. D., *Acta Cryst.* **B29,** 2433 (1973).
24. Schuit, G. C. A., *J. Less Common Metals* **36,** 329 (1974).
25. Kumar, J., and Ruckenstein, E., *J. Solid State Chem.* **31,** 41 (1980).